5.10 Machine Detector Interface

5.10.1 Overview

The Beam Delivery System at CLIC will have a single interaction point where two detectors will be alternated to share the beam time in a so called "push-pull" mode. The two experiments will alternate between their data-taking and garage positions, moving by ~30 m on independent platforms equipped with air pads or rollers and alignment features.

In and around the detector region a number of accelerator components are necessary for proper machine operation and in particular for luminosity optimization. One of the driving elements is the final focusing quadrupole QD0, which serves to provide the small vertical beam spot of 1 nm r.m.s.. The distance L* of the downstream end of this quadrupole to the interaction point must be minimised to allow as strong focusing as possible. In the present layout L* has been chosen to be 3.5 m, implying that the quadrupole is mounted inside the detector. The required strong gradient is achieved with a hybrid magnet composed of permendur, reinforced with permanent magnets, and with additional and tunable field strength provided by coils, as described in sections 2.6.3.1 and 5.10.21.

Any movement of the quadrupoles with respect to the beam would affect the transverse position of the beam at the interaction point by a comparable amount. Therefore for frequencies above 4 Hz its position must be stabilized to 0.15 nm r.m.s. in the vertical plane to ensure that the luminosity loss due to this effect is kept below the two percent level. The stabilization of the QD0 is hence one of the main challenges in CLIC.

Multiple approaches have been introduced to ensure this stabilization level at the IP, namely: (1) incorporating a robust active pre-alignment system crossing the detector, (2) adopting a permanent magnet arrangement for the QD0 quadrupoles to prevent vibrations due to cooling, (3) supporting the QD0s from stable mechanical supports mounted off pre-isolator masses so as to be completely decoupled from technical noise produced by the detector, and (4) providing an active stabilization system for the QD0s. A laboratory set-up has demonstrated that the 0.15 nm stability level (at 4 Hz and above) can be reached if the stability of the mechanical QD0 support is better than ≈ 5 nm. In addition, recent measurements in the CMS experimental area have shown that, in a well-designed underground experimental area, this value can be reached. Although the results obtained to date are very encouraging, work must be continued to integrate all of the needed elements within the limited space available, as well as to demonstrate their performance in the stray field of the main experimental solenoid, and in the CLIC radiation environment.

This is achieved by mounting the quadrupole inside a rigid support tube, mounted on a massive pre-isolator, described in section 5.10.2.3, which also holds the horizontally focusing quadrupole QF1 and some higher order chromatic corrector magnets. Inside the support tube the magnet position is mechanically stabilized by a continuously active system based on capacitive sensors and piezo-actuators, described in section 5.10.2.2. Mechanical structures are, wherever possible, optimized to have their first resonances around (multiples of) the 50 Hz machine frequency.

An active pre-alignment system ensures that the average position is corrected to within 10 μm r.m.s. with respect to the Beam Delivery System elements and with respect to the other QD0 magnet. Special channels for laser light have been reserved through the detector to allow monitoring of the relative QD0 positions, as described in section 5.10.2.4.

Complementing the mechanical stabilization system, the intra-pulse feedback system (section 5.10.2.5) measures the position of the outgoing beam and applies a calculated kick to the other incoming beam to optimize the luminosity. Although bunch-to-bunch correction is not possible, the latency time of this feedback loop is small enough to allow several iterations within one 156 ns bunch train. As described in section 2.6.3.4 this may lead to a significant improvement of the mean luminosity. Further feedback and feed-forward systems are implemented in the main linacs and beam delivery systems to ensure beam stability for frequencies below 4 Hz.

The vacuum pressure requirements are not excessively challenging in the machine interface region, but the vacuum system layout is challenging due to requirements for the operation of the two detectors in push-pull mode. Access must be provided to the vacuum valves that separate the sections and the time for pumping after changes of detector must be minimized. The vacuum strategy and layout is described in section 5.10.2.7 and the accessibility issues are an important part of the overall integration as described in section 5.10.2.8.

Finally the detectors must be located in suitable caverns with infrastructure and services. In section 5.10.2.9 we describe the requirements for the civil engineering and services and the suggested approach to cover these needs. Figure 1 shows a general view of the CLIC interaction region.

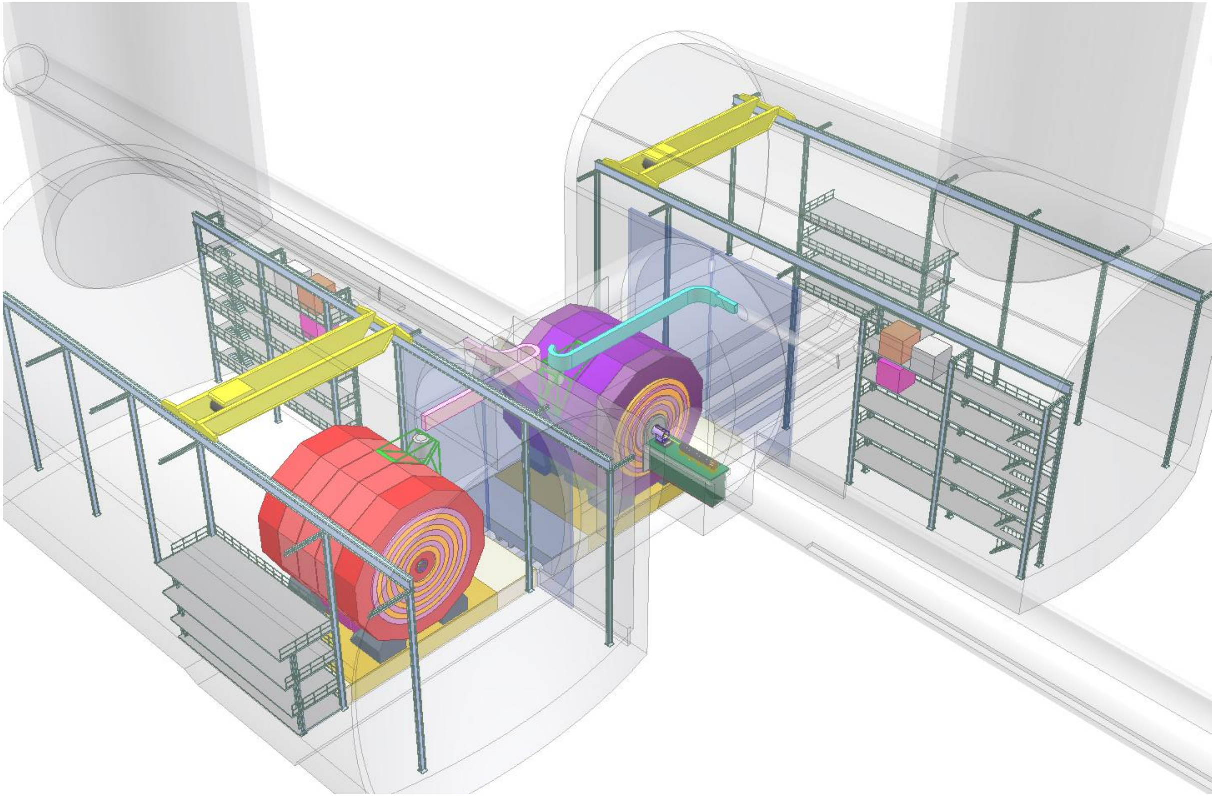

Fig. 1: General view of the interaction region at CLIC

5.10.2 Technical description

5.10.2.1 QD0 magnet assembly

5.10.2.1.1 Magnet Design

Due to the specific layout of the CLIC Machine Detector Interface (see Section 2.6.3.1) the space for the QD0 magnet is quite limited in the horizontal plane but not so much in the vertical one. For this configuration it seems advantageous to adopt a classical “8” (or “two leaves”) quadrupole design. Figure 2 shows the conceptual design of the proposed cross-section for the QD0 magnet. The “8” design is easily recognizable; the electro-magnetic (EM) coils are placed on the top and bottom return steel yokes.

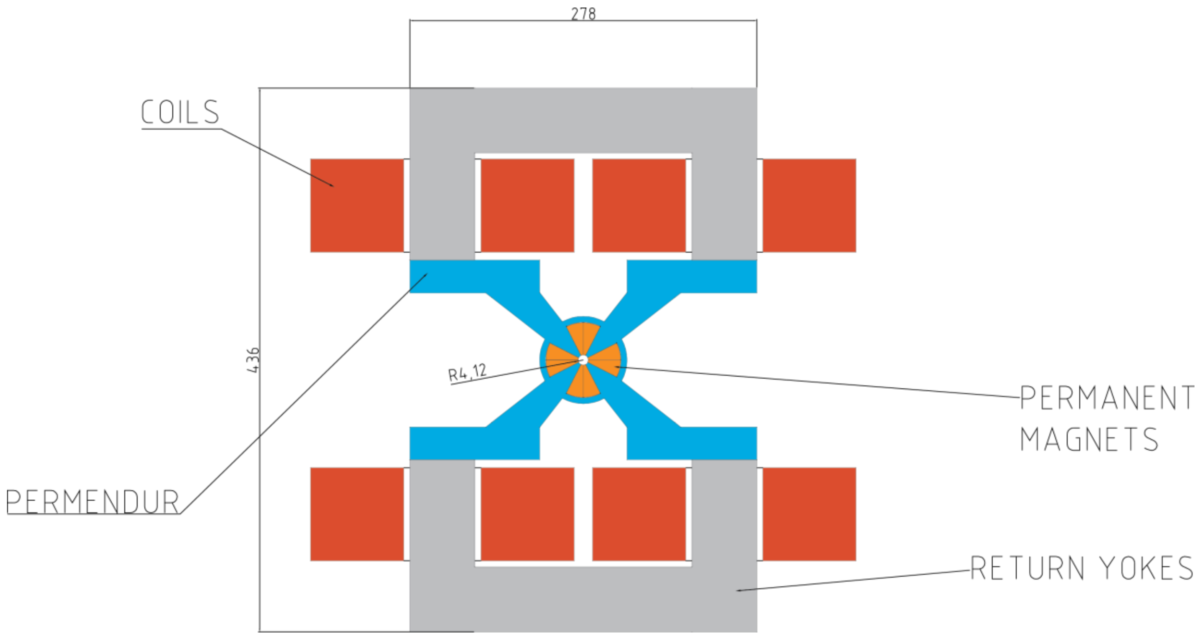

Fig. 2: Conceptual design of the QD0 cross-section

A limitation for the maximum strength achievable in an iron-dominated quadrupole magnet is given by the saturation of the poles and by the pole shape-factor that causes, above a certain gradient and saturation, a "short circuiting" of the magnetic flux lines across the poles outside the magnet aperture.

To limit this effect and to increase the maximum achievable gradient, 4 blocks of permanent magnet (PM) with adequate magnetization directions are added to the structure between each pair of poles. Each one of the 4 PM blocks is composed of two parts with different magnetization directions. It must be noted that the PM blocks are not actively contributing to the quadrupolar magnetic field in the magnet bore, but they act mainly to optimize the magnetization inside the iron poles. They compensate spurious magnetic components that are not useful for building up the magnetic gradient in the aperture but that would add only to the saturation of the poles and the "short circuits" between them [1].

The ring-like structure that links the four poles has been added for structural reasons; high magnetic forces will be generated in the structure when it is powered, while magnetic field quality will be strongly dependent on the precise geometry of the poles. The presence of the ring, built-in during the pole machining (by a wire-erosion process), should guarantee the mechanical stability and hence the correct geometry. A drawback of the ring is the short-circuiting of some magnetic flux that will cause a reduction of gradient inside the magnet aperture by approximately 20 T/m.

In order to achieve higher gradient values the central part of the structure is made of "permendur", a Fe-Co alloy characterized by a high magnetic saturation level compared with classical low-carbon magnetic steel. Depending on the type of permanent magnet material chosen (among the SmCo or NdFeB families) the maximum gradient expected (with coils powered at 5000 A·turns) are:

~ 530 T/m (with Sm_2Co_{17})

~ 590 T/m (with $Nd_2Fe_{14}B$)

We recall that the nominal gradient is 575 T/m as reported in Table 2.2, see Section 2.6.3.1.

The EM coils will work at very low current density (~1.0 A/mm^2). This avoids the use of an active cooling system of the coil pancakes, which is a very positive aspect from the point of view of vibrations of the structure, relevant for the QD0 stabilization (see section 5.10.2.2).

Varying the current from zero to 5000 A·turns corresponds to varying the gradient between ~50 to ~590 T/m and permits a wide tunability of the magnet. The use of 4 independent power supplies should allow for compensation of potentially small differences between the pole performances (due to PM block tolerances, reproducibility, and to mechanical errors or deformations).

In Figures 3 and 4 we show the magnetic induction of the structure with coils powered at 0 (Figure 3) and 5000 A·turns (Figure 4), respectively. The major difference in the magnetization (in strength and direction) of the magnet poles should be noted.

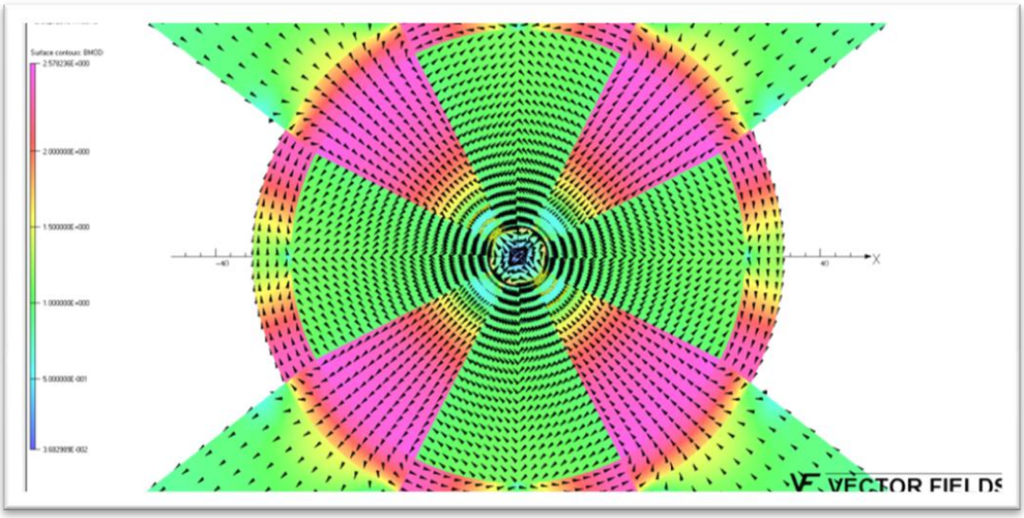

Fig. 3: Magnetic behaviour of the magnet with 0 A·turns in the coils (the gradient in the magnet bore is in this case ~ 50 T/m)

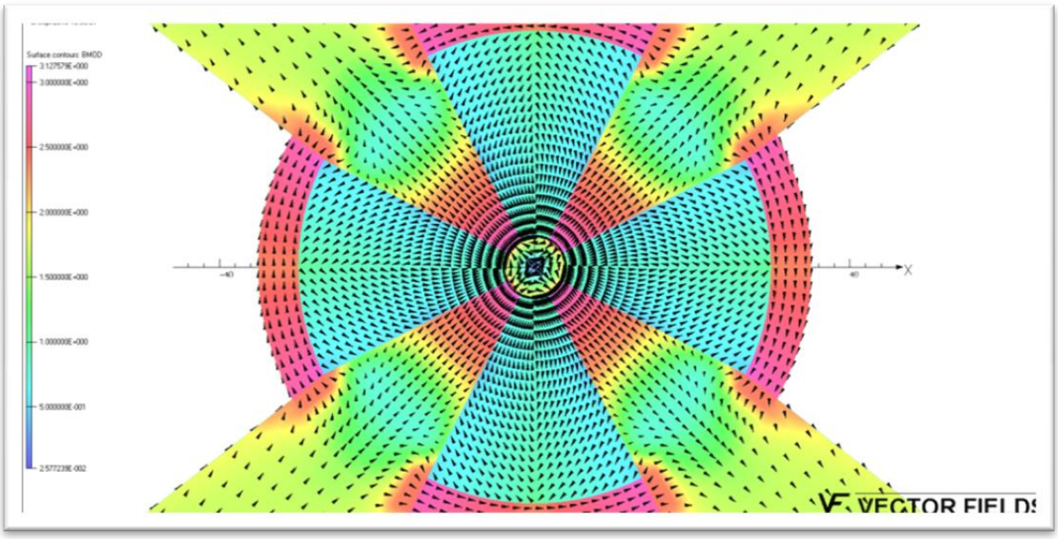

Fig. 4: Magnetic behaviour of the magnet with 5000 A·turns in the coils. (Gradient in the magnet bore is ~ 530 T/m)

5.10.2.1.2 Short prototype

A prototype model with full-scale cross-section, working at nominal conditions, but with much shorter length (full QD0 length: 2730 mm), is under construction [2]. A view of the prototype is given in Figure 5.

The aims of this prototype are:

- To validate the concept of the "hybrid magnet",
- To check the behavior of PM blocks of different materials working under an external high magnetic field generated by the EM coils (note: The PM blocks will be easily dismountable),
- To check the mechanical soundness of the assembly, a critical aspect for the required field quality,
- To provide a real "case study" for the development of new magnetic measurement systems (by rotating coils compatible with 7-8 mm diameter magnet aperture) actually under development at CERN.

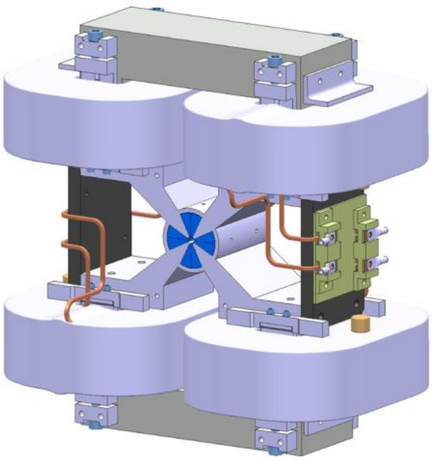

Fig. 5: Hybrid QD0 short prototype

5.10.2.1.3 Toward a Final Magnet Design

The major differences between the proposed cross-section for the short prototype and the one for a longer version that is supposed to work in the real MDI environment are (see Figures 6 and 7):

- Even if the coil will work at a very low current density (~ 1.0 A/mm^2), for a longer structure installed in a very confined environment, like the MDI, control of the temperature must be foreseen. For this reason, and also in order to give more stiffness to the coil assemblies, we intend to include in the coil pancakes some longitudinal bars (of non-magnetic metal) in order to allow the cooling (or more precisely, the thermalization) of the coils.
- The coils can be supported independently of the magnet core. This will simplify the active stabilization scheme since the coils are the heaviest part of the magnet assembly and the cooling water flow will not directly affect the magnet core, for which the active stabilization must be guaranteed.

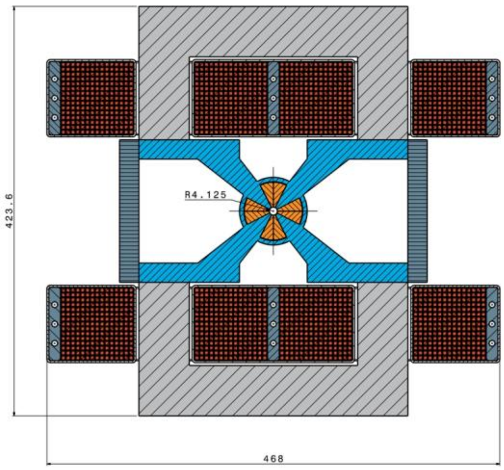

Fig. 6: QD0 with thermalization coils

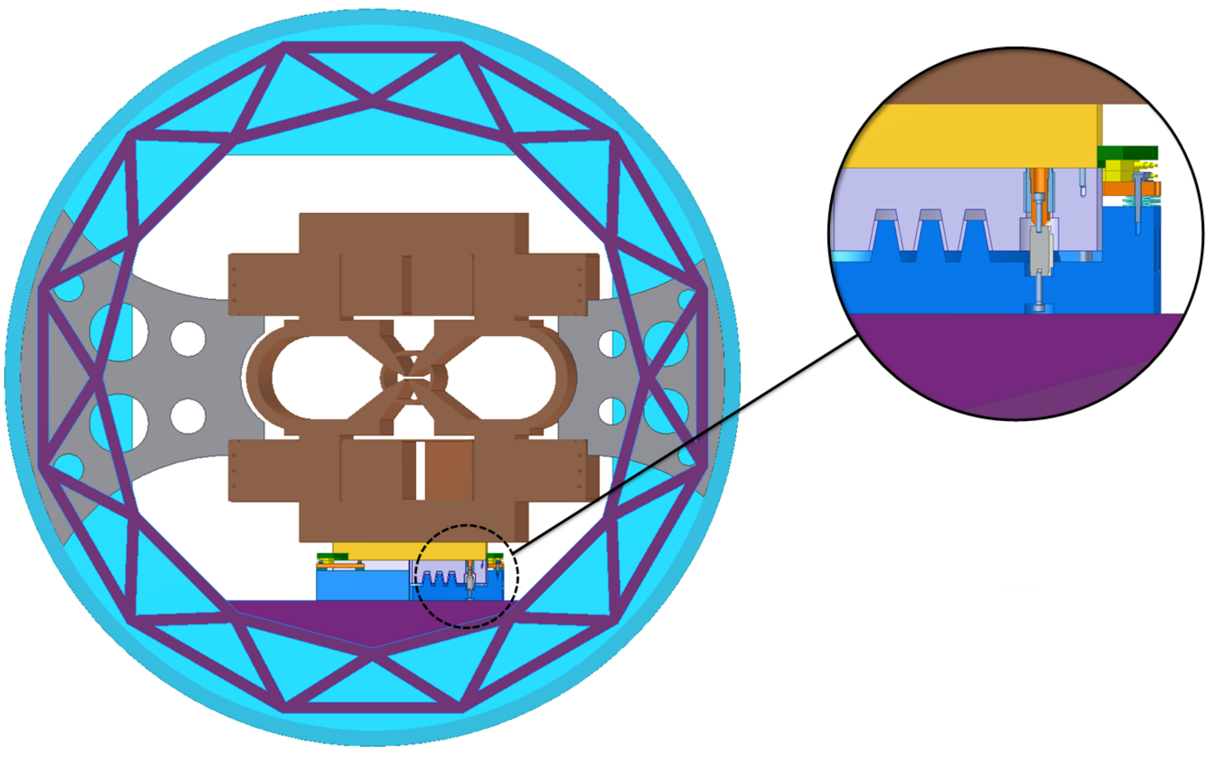

Fig. 7: Magnet/coils independent support. The integration of the stabilisation foot in the support is shown in more detail on the right hand side.

The stabilization needs and studies will require identification of the fundamental mechanical characteristics of the structure (fundamental resonance frequencies, intrinsic structure stiffness, etc.). As an example, Figure 8 shows the first resonance frequency and oscillation mode for a structure in which the return yokes are composed of single "Steel 1010" pieces but the core part (made in permendur) is composed of 27 elements of 100 mm individual length (this is a possible solution if manufacturing by the wire-erosion technique of these components is retained).

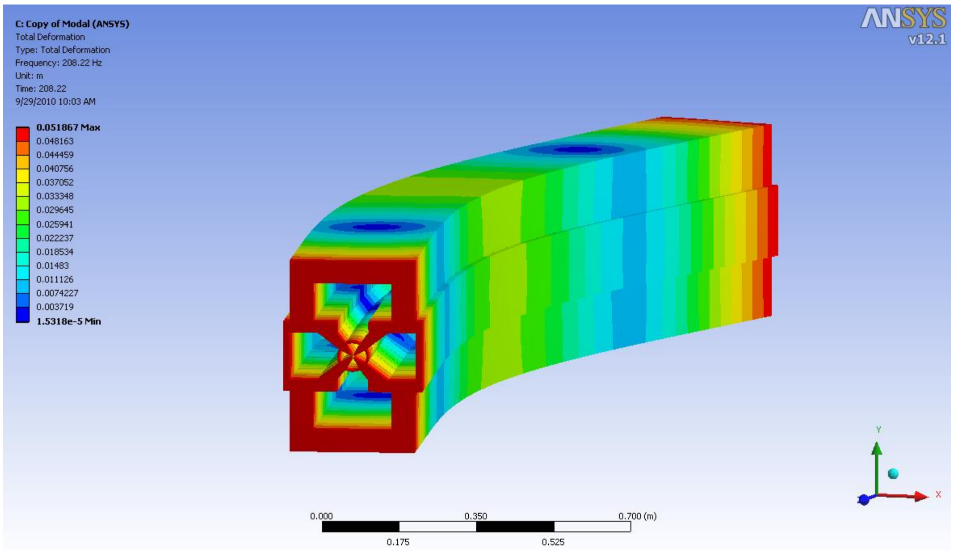

Fig. 8: 1st resonance frequency and oscillation mode for a full-length QD0 core assembly

5.10.2.2 QD0 stabilization

The very strong gradient of the QD0 quadrupoles, necessary to produce the extremely small vertical beam spot size of 1 nm r.m.s., has the side effect that any offset between the axis of the quadrupole and the beam trajectory leads to a displacement of the beam at the interaction point by a comparable amount. To avoid luminosity loss the vertical position of the quadrupole must therefore be stabilized to 0.15 nm r.m.s. for frequencies of 4 Hz and above. This will be achieved by an active stabilisation system, complemented by a passive pre-isolator (see section 5.10.2.3) and beam based feedbacks (see section 5.10.2.6). The stabilization of the QD0 quadrupoles is indeed one of the main challenges in CLIC.

For an active stabilization system to work in the harsh and crowded environment of the final focus section, one needs to measure vibrations and find a strategy for counteracting the undesirable vibrations by acting on QD0 to obtain the required stabilization in the vertical direction. Sensors and actuators are needed that are compact, light compared to the QD0 weight, resistant to magnetic fields (QD0 being inside the detector solenoid) and resistant to radiation, and that can function at the sub-nanometer scale in the frequency range from 0.1Hz to 100Hz. A large number of sensors have been studied [3] and several geophones, piezoelectric and chemical sensors have been identified as possible candidates. Piezoelectric actuators are suitable for this application. Stabilization to the sub-nanometre level has been proven to be feasible using commercial equipment on a simplified QD0 prototype. A stabilization of 0.13 nm r.m.s. at 4Hz has been achieved in the laboratory at the extremity of a cantilevered prototype where the initial displacement is maximal, see Figure 9 [4, 5].

The strategy chosen so far for this performance has been to isolate QD0 from ground motion with a large commercial table combining passive and active isolation, with the addition of an extra feedback on QD0 to compensate for the structure resonances. A study is now underway to replace the commercial stabilization system by a more compact device, the current test set-up having the following dimensions: 24x24x5cm^3. The lower part is dedicated to a rigid stabilization table equipped with 4 actuators that allow movements in 3 degrees of freedom with integrated relative capacitive gauges and elastomer for movement guidance [6]. Figure 10 shows a preliminary design of such a device. The passive part of the stabilization scheme is still under investigation. In any case the stabilized support will be mounted on a passive pre-isolation system, described in section 5.10.2.4.

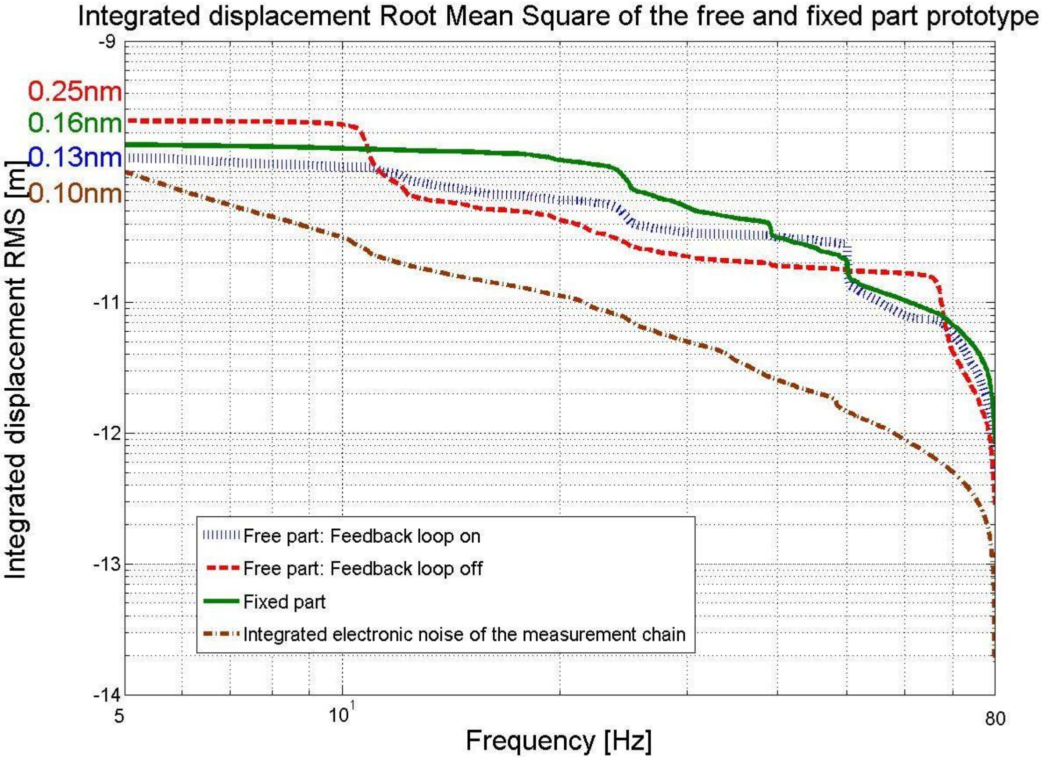

Fig. 9: Stabilization of a QD0 prototype to 0.13 nm for frequencies above 4 Hz.

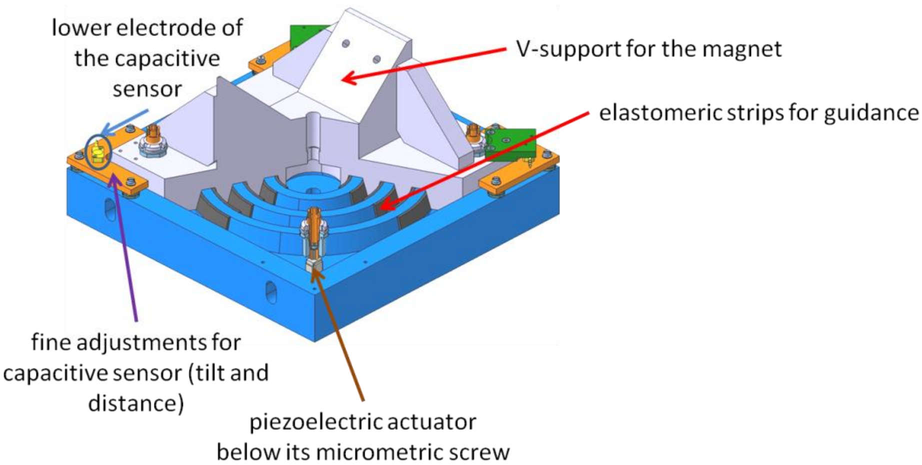

Fig. 10: Preliminary design of a stabilization device.

Since this compact device only stabilizes in a relative manner, an absolute sensor like the ones used for the QD0 prototype study will have to be added to the magnet support.

Calculations are under way to determine the best longitudinal locations for the isolation device under QD0, taking into account the positions where maximal compensation is needed, the restricted space available and cost. For lack of space, one might be forced to adapt a cantilevered support scheme. A possible integration below the QD0 magnet, with stabilization systems at the Gauss points, is shown in Figure 7.

In order to limit the number of stabilization components, it is necessary to design QD0 in order to minimize vibration induced by technical noise; thus the luminosity calorimeters and QD0 coils will be supported independently. The whole support is mounted on a pre-isolator that is described in the next section.

In addition, QD0 stabilization will need to be complemented by a combination of active and passive systems to minimize beam jitter and finally the beam position will be corrected by a an intra-pulse feedback system to maximize CLIC performance as described in section 5.2.10.6. In previous studies the overall performance was clearly limited by the linear controller characteristics. An adaptive controller has been designed and combined with stabilization devices that have passed feasibility performance. Recent simulations show that a performance of 0.02 nm r.m.s. at 0.1Hz should be sufficient. However, to achieve this performance, the integrated sensor noise should correspond to below 0.13 pm r.m.s. at the IP at 0.1Hz, i.e. 0.13 μm at the BPPM. Whatever system or combination of systems is chosen for CLIC, it should comply with the model shown in Figure 11. This curve specifies what is needed to obtain the desired stabilization performance [6]. The calculated transfer function for the final quadrupoles has been included in the integrated beam dynamics simulations, see Section 1.5. The simulations show a good performance even for relatively noisy sites.

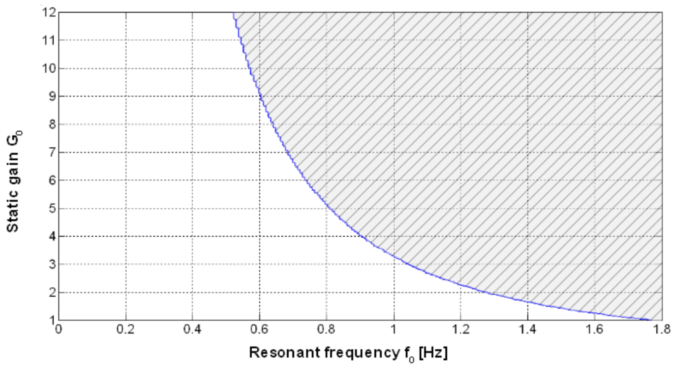

Fig. 11: Pattern for an active/passive isolation system for CLIC if the stabilization criterion is to be met. The isolation system studied is a 2nd order low-pass filter characterised by 3 parameters: the static gain, the resonant frequency and the damping factor. The pattern shown is taken in a domain where it is independent of the damping factor.

5.10.2.3 QD0 and QF1 pre-isolation

The ground micro-seismic motion at frequencies above 4 Hertz, either natural or generated by machinery, can be effectively reduced by a passive mechanical low-pass filter [7]. A simple one-dimensional spring-mass system, with its first resonant frequency at $f_0 = (1/2\pi)\cdot(K/M)^{1/2}$ Hz, where K is the spring constant and M the mass, shows a transfer function similar to Figure 12.

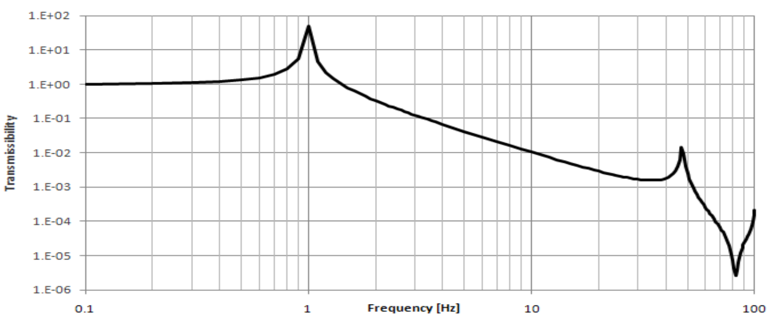

Fig. 12: Transfer function of a spring-mass system tuned at 1 Hz.

At frequencies below f_o, the ground motion is transmitted to the mass without any attenuation whilst at frequencies above f_o, the motion of the suspended mass is attenuated by a factor $(f/f_o)^2$. At frequencies close to the resonance the motion can be amplified and a damping system is usually required. In reality, at higher frequencies, other resonances internal to the spring and the mass appear. They do not affect the attenuation performance, but rather limit the effective frequency bandwidth.

In the case of the CLIC final focus complex, with the QD0 and QF1 doublet, the layout represented in Figure 13 is proposed. The common support ensures that QD0 and QF1 move coherently.

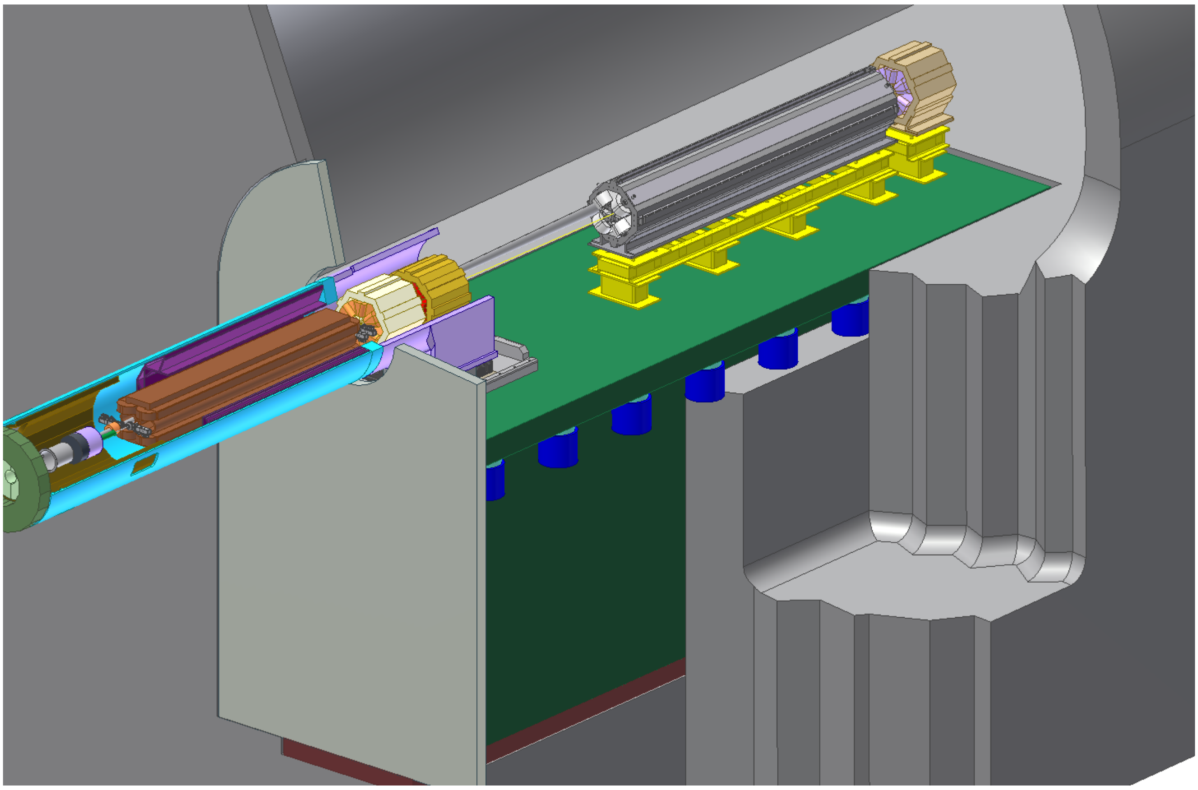

Fig. 13 – Layout of the pre-isolator, with the concrete mass supporting the two final focus quadrupoles QD0 and QF1.

The two magnets are supported by rigid girders that are fixed on top of a massive concrete block, weighting about 80 tons and resting on several springs (in blue in Figure 13) whose rigidity is tuned in order to have a vertical resonance of the whole assembly at 1 Hz. Vertical ground motion at frequencies below 1 Hz just by-passes the pre-isolator, without being attenuated or amplified; ground motions at frequencies above 1 Hz are reduced by a factor f^2 up to the first internal resonant mode, which can be tuned to be in the bandwidth 30 – 50 Hz.

The system is designed to provide a reduction of the r.m.s. vertical displacement from about 3 to 0.1 nm at 4 Hz and it has to work in combination with the pre-alignment and the active stabilization, of which it actually constitutes the first element.

5.10.2.4 QD0 pre-alignment

The final doublet quadrupoles must be pre-aligned very precisely for the luminosity optimization procedure to converge. The pre-alignment solution proposed for the MDI must fulfill the following requirements:

(1) Determination of the transverse position of QDO with respect to the other components of the last 500 meters of the Beam Delivery System (BDS), within 10 μm r.m.s.; longitudinally this requirement is 20 microns r.m.s. between QD0 and QF1;
(2) Monitoring of the position of one QD0 with respect to the other QD0 within 10 μm r.m.s.;
(3) Determination of the position of the left side components with respect to the right side components of the tunnel within ±0.1 mm r.m.s.;
(4) Remote and high-resolution (sub-micrometric) re-adjustment solution.

The approach can be summarized as follows:

(1) The solution chosen for the determination of the position of the Main Beam quadrupoles [8] has been adopted. The strategy proposed is first to measure the mechanical zero position of QD0 with respect to the sensor mechanical interfaces on a Coordinate Measurement System (uncertainty of measurement below 1 micron) in a stable and controlled lab. Once in the tunnel, QD0 will be equipped with 2 Wire Positioning Systems (WPS) and one inclinometer with 2 axes, installed on the measured mechanical interfaces (see Figure 14). The WPS will determine the position (radial, vertical, yaw and pitch) of QD0 with respect to a stretched wire. The 2-axis inclinometer will provide the roll information as well as a redundancy in the pitch axis. The main difference with respect to the main linac quadrupoles concerns the Metrologic Reference Network (MRN) used to define the straight line of pre-alignment. In the BDS case, the length of the last wire will be 500 m, with no overlap in the last 250 m, due to space constraints. For the same reason, the Hydrostatic Leveling System (HLS) needed for the modeling of its sag will not be extended up to QD0. The catenary of the wire will have to be extrapolated in the last few meters of the tunnel.

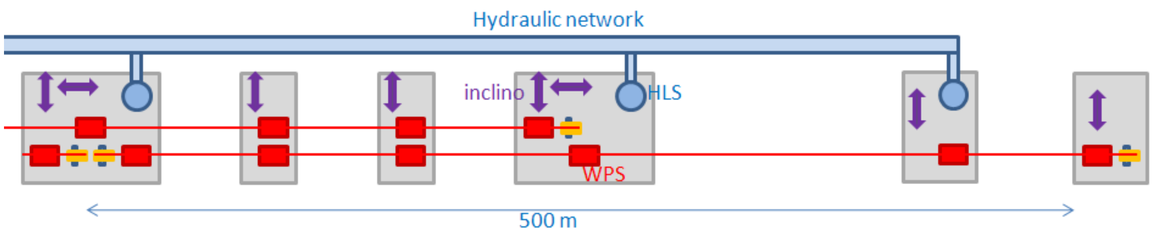

Fig. 14: Schematic layout of the pre-alignment equipment in the last 500 m of the tunnel.

The determination of the relative longitudinal position of QD0 w.r.t. QF1 will be performed using capacitive sensors, with sub-micron precision, coupled to each component, measuring without contact the distance towards targets located at each end of a calibrated carbon bar.

The position of the two QDOs (left and right), will be monitored by a network of over-determined nodes; each node consists of a combination of RASNIK [9] systems that allow measurements through the detector, using the dead space between polygons (in the calorimeters) and circular detector areas (in the trackers), see

Figure 15. Each node will be a combination of RASNIK systems, calibrated with sub-micron accuracy:

- "standard" RASNIK systems, consisting of 3 separate elements: a mask, back-illuminated by LEDs, imaged through a lens onto a CCD acting as a screen;
- RASNIK proximity cameras, with CCD and lens coupled together in a solid camera body.

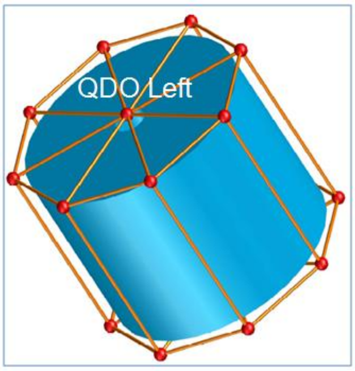

Fig. 15: Schematic layout of RASNIK nodes.

(2) The BDS are like 2 antennas around the IP and the "ideal straight lines" will have to meet at the IP. Some permanent monitoring systems will provide the relative position of the two antennas, within ±0.1 mm. The same principle as in the LHC is proposed: the spatial distances of the two reference lines of the Beam Delivery System (stretched wires) to a common reference line (a wire stretched in a parallel dedicated gallery) will be determined 3 times on each side. Survey galleries and boreholes between the galleries and the tunnels will host the alignment solutions.

(3) The remote and high-precision readjustment solution is the same as the one foreseen for the Main Beam quadrupoles: cam movers are proposed for the 5 degrees of freedom (DOF) readjustment of QD0. The eccentric cam-based adjustment system is a 3-point system, with 4 interfaces with the settlement, providing 5 DOF. This system, which supports also e.g. the girders of the Swiss Light Source at PSI and the undulators of the XFEL at SLAC, is used in several other accelerators or synchrotrons, but not with the sub-micron resolution of displacement required for CLIC. The only modification with respect to the main linac quadrupoles concerns the additional remote adjustment of the longitudinal axis, performed using a stepper motor.

5.10.2.5 Push-pull system

The two detectors CLIC_ILD and CLIC_SiD have a similar layout, based on a superconducting solenoid and an iron return yoke consisting of massive end-caps and a barrel region split longitudinally in three rings. This concept allows a surface assembly with pre-commissioning of the solenoid, followed by independent lowering of the rings in the underground cavern in the same way as was done for the CMS detector. The central ring of the barrel will support the cryostat of the superconducting coil. The calorimeters and the tracker are situated within the free bore volume of the vacuum tank. The differences in the two layouts come from the peak magnetic field, the free bore (diameter of the coil), the choice of the inner detector technology and a different L*. Figure 16 shows the main dimensions of CLIC_SiD and CLIC_ILD.

The thickness of the yokes is defined by the requirements for magnetic self–shielding to reduce the fringe field but also for radiation self-shielding to limit the dose to personnel in the cavern during data-taking as well as limit doses in case of an accidental beam loss. It can be noted that compact detectors in a short experimental region also have a very efficient radiation shielding scheme.

In addition the thickness of iron in the movable parts (doors) of the endcaps is constrained by requirements of compactness along the beam line, to accommodate the required L* and to provide vibration immunity of the QD0s by keeping their support tubes as short as possible. For this purpose equipping the longer experiment (CLIC_ILD) with end-coils [10] is being considered, so as to reduce its length to match the 12.80 m overall length of the CLIC_SiD detector, while still providing the same level of fringe field.

Figure 17 shows the QD0 magnet with the different sections of vacuum tank and separating valves. These valves are very important for opening the detectors and for push-pull operation.

Both detectors have an approximate weight of the order of 13000 tons dominated by the weight of the iron yoke with an overall height of 14 m and a total length along the beam of 13 m. Table 5.10.1 summarizes the main parameters.

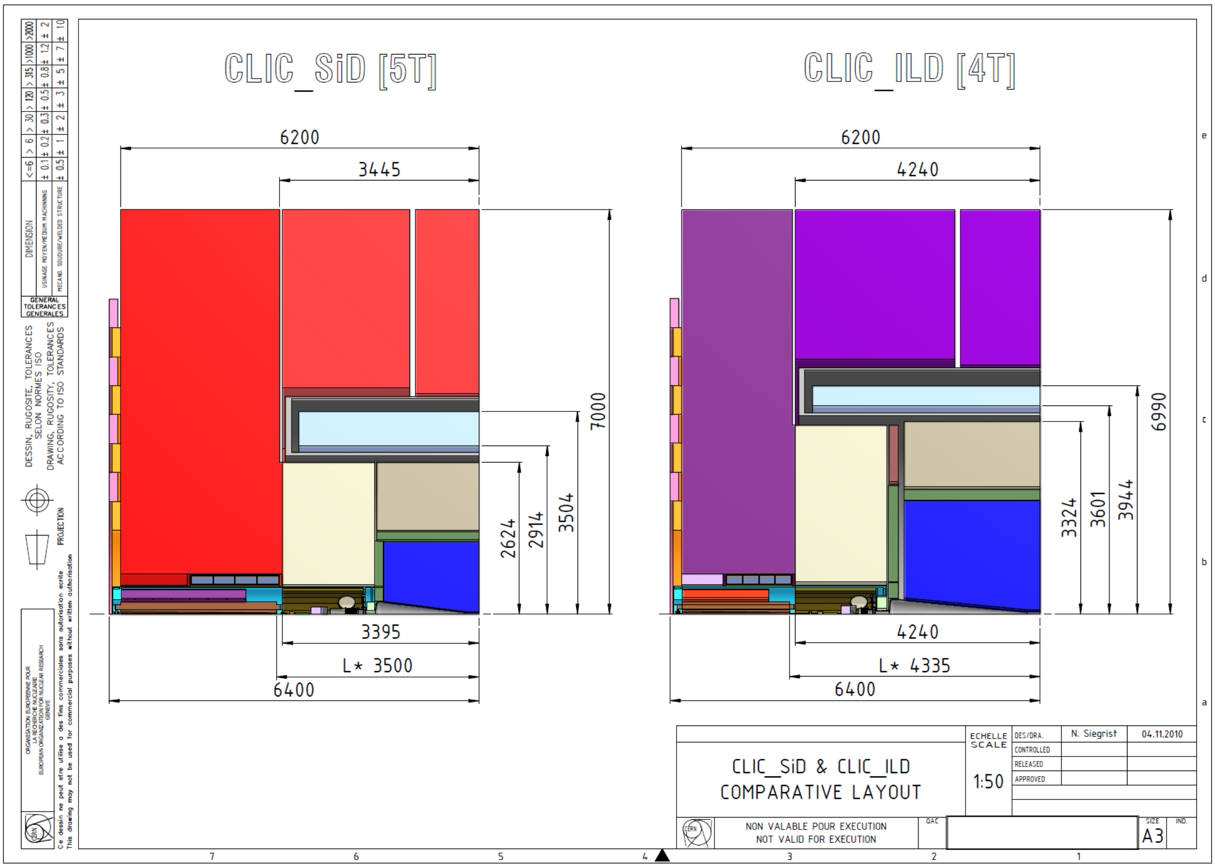

Fig. 16: Quarter views of the two basic detector layouts of CLIC_SiD and CLIC_ILD

In push-pull operation, while one detector is taking data on the beam, the other will be in its garage position. This imposes shielding constraints for the protection of the working personnel against exposure to the magnetic fringe field and to the radiation dose induced by accidental beam losses. The distance between the two detector axes along the push-pull direction is 28 m, while 15 m is the distance from the beam axis to the beginning of the garage area in the experimental cavern.

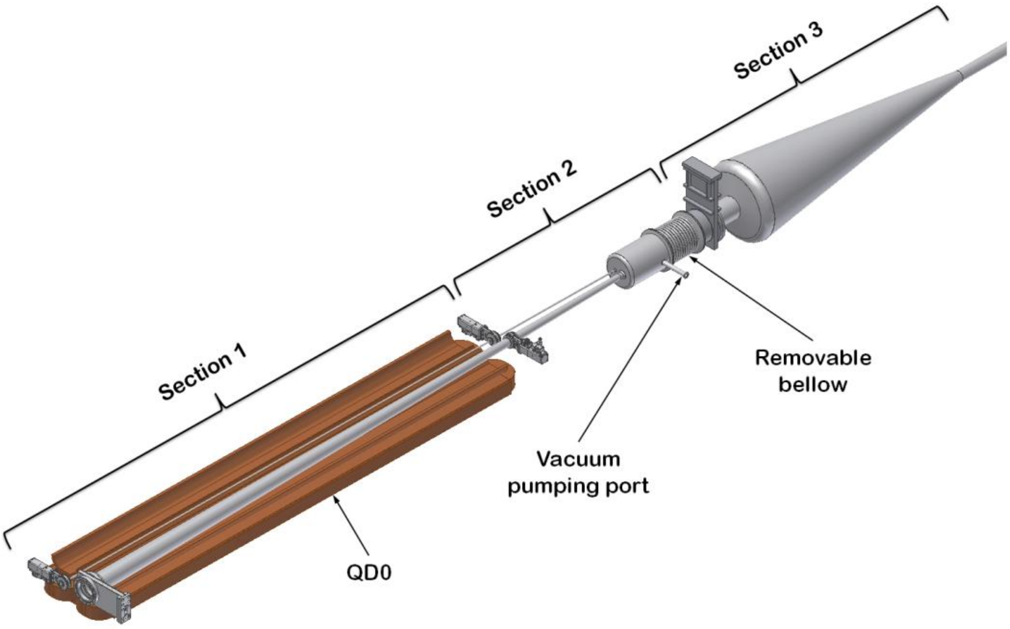

Fig. 17: View of QD0 magnet and vacuum sections and valves

Table 5.10.1: Main dimensions and weights

Parameter	CLIC_SiD	CLIC_ILD with end-coils
Detector length	12.40 m	12.40 m
Overall length with shielding rings	12.80 m	12.80 m
Detector diameter on flat	14 m	13.98 m
Free bore	5448 mm	6852 mm
Coil inner diameter	5828 mm	7202 mm
Coil outer diameter	7008 mm	7888 mm
Coil length	6230 mm	7890 mm
L*	**3500 mm**	**4340 mm**
Bore in Endcap for support tube and anti-solenoid	1380 mm	1380 mm
Radial height vacuum tank	1020 mm	828 mm
Vacuum Tank length	6690 mm	8350 mm
Coil weight	201 tons	173 tons
Vacuum tank weight	128 tons	173 tons
1 Endcap weight	2900 tons	2100 tons
Barrel weight	5000 tons	4700 tons
Complete return yoke	10800 tons	9900 tons
Detector total weight	**12500 tons**	**11800 tons**

Measurements of the stray field in the CMS experimental cavern have shown [11] that work is becoming more difficult in stray fields exceeding 50 Gauss. Therefore the return yoke must be designed to be self-shielding to ensure that 50 Gauss is not exceeded at a horizontal distance of 15 m from the beam axis. Magnetic self-shielding is also important when the off-beam detector performs magnetic tests in its cavern. These tests should not distort the field map of the on-beam detector by more than 0.01% inside its tracking volume (ILC criteria).

The concern of maximum exposure to ionizing radiation for personnel working in the cavern during beam operations comes from potential beam losses. The iron yoke itself will provide enough shielding for beam losses inside the detector, but one of the most likely locations where losses happen is in the region of the final focus magnets, at the interface between the end-cap and the cavern wall. For this case, shielding is provided by concentric shielding rings on the backside of the end-cap iron, interleaved with shielding rings that are fixed on cavern wall. The latter can be moved in and out by pneumatic or hydraulic jacks, thus creating a chicane system that closes perfectly the gap between the end-cap and the tunnel wall. Figure 18 shows the detail of the chicane system for radiation shielding. Simulations show that such a system will keep the radiation dose at very acceptable levels even if a full bunch train is lost on the QD0 magnet.

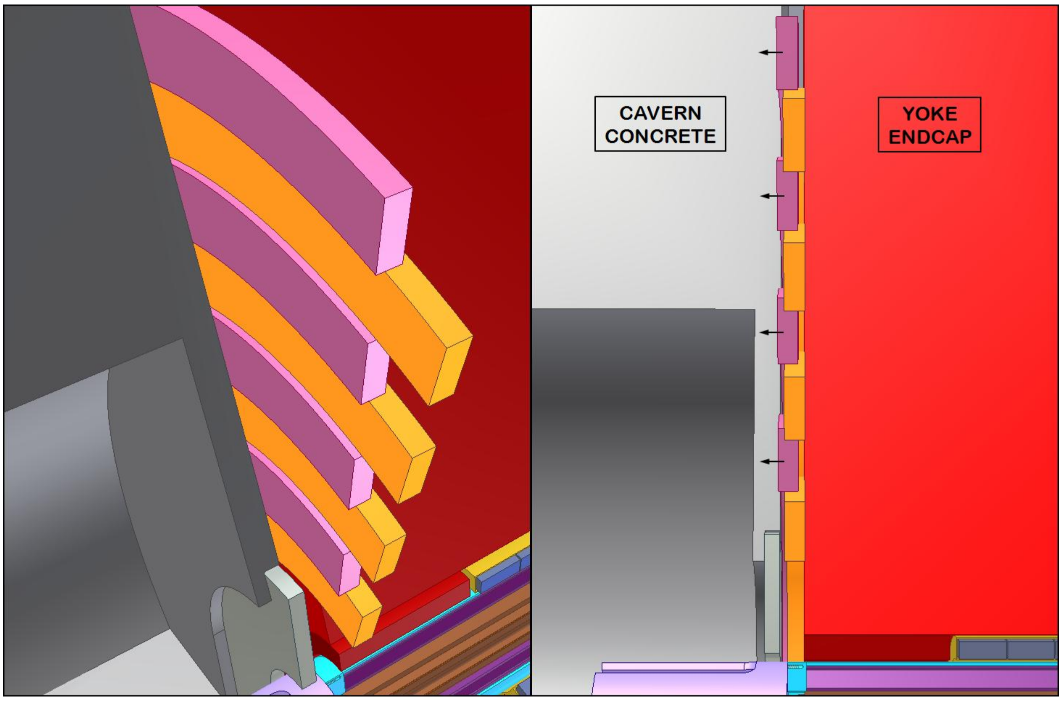

Fig. 18: radiation chicane made of concentric ring modules

5.10.2.6 Intra-pulse feedback system

The beam-based IP intra-train feedback (FB) system was outlined in Chapter 2.6.3.4. The schematic layout of the components is shown in Figure 19.

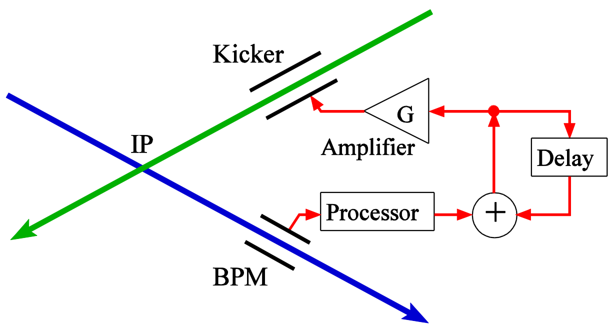

Fig. 19: Schematic layout of the IP feedback components

Prototypes of the BPM, signal processor, feedback circuit, kicker and drive amplifier have been developed and tested with beam by the FONT collaboration [12,13,14]. Key parameters are the latency of the components, which impacts upon the luminosity recovery potential, and the drive power of the amplifier, which determines the angular deflection that can be given to the beam. It is assumed that a short (approx. 10 cm long) stripline BPM will be used to provide a fast input beam position signal, and a short (approx. 25 cm long) kicker will be used to provide the correcting beam angular deflection. These are compact, intrinsically fast, high-bandwidth components of 'standard' design. Actual devices with geometries optimised for the tight space constraints of the CLIC IR will need to be engineered as the IR design evolves. For the layout shown in Figure 19, with the BPM and kicker located approximately 3m from the IP, the beam round-trip time of flight delay is about 20 ns.

A prototype BPM signal processor has been designed (Figure 20a), with micron-level resolution, and a latency of 5ns has been demonstrated [13]. A high-power kicker drive amplifier that meets CLIC requirements has been built (see Figure 20b) and tested with beam at ATF [14]. In order to optimise the latency the feedback circuit was integrated into the amplifier board; a combined (feedback circuit + amplifier + kicker rise-time) latency of 8 ns was measured [14]. Assuming these demonstrated prototype latencies yields a total system latency of 33 ns. For the FB performance simulations described in Chapter 2.6.3.4 a latency of 37 ns was assumed, which allows an extra 4 ns of delay, for additional cabling and/or adjustment of the electronics location near the IP. With further optimisation of the component locations and cabling, and development of faster electronics, a total latency as low as 30 ns may be achievable.

a)

b)

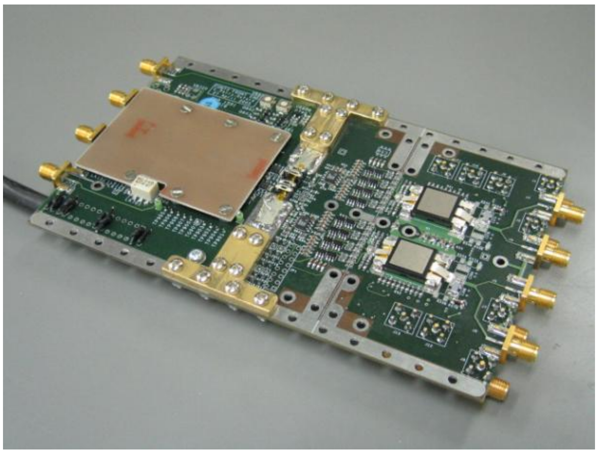

Fig. 20: Prototype modules for the IP Feedback system: a) BPM signal processor, b) integrated feedback circuit and drive amplifier

5.10.2.7 Vacuum system

The MDI baseline is a non-baked system using ultra-high vacuum (UHV) materials and procedures to obtain the pressures specified in section 2.6.3.5. The layout of the QD0 magnets limits the chamber diameter to 7.6 mm and pump separation to ~4 m. Assuming a clean, unbaked vacuum system, a static pressure profile after 100 hours of pumping has been calculated (see Figure 21). This corresponds to an average pressure of 3.6x10^{2} nTorr. This conforms with the requirement of beam-gas background, but gives little margin for additional beam-induced outgassing. The QD0s should therefore be kept under vacuum to minimize contamination with water vapor.

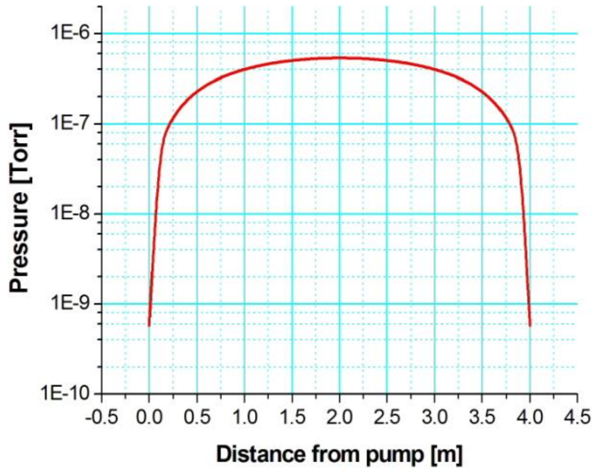

Fig. 21: Static pressure profile in QD0 region after 100 hours of pumping.

The MDI region is planned to be physically sectorised with ultra-high vacuum valves as shown in Figure 22. Two valves are required in the space between QD0 and the experiment to allow the detectors to be exchanged (push-pull) whilst maintaining the QD0 and experimental beam pipe either under vacuum, or filled with a clean, inert gas. The post-collision line is separated from the collider beam line to allow independent interventions to these sectors. A fast shutter may be installed on each post-collision line to prevent contamination of the experimental sector due to incidents in the post collision line.

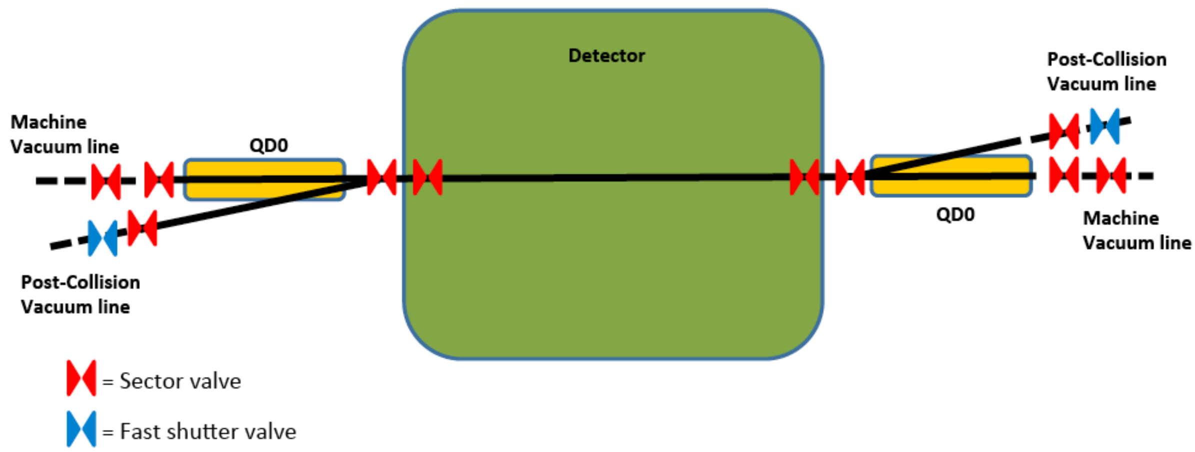

Fig. 22: Sectorisation of vacuum in MDI region

Each of the sectors (QD0, experimental, post-collision) will require a self-contained system of pumps and vacuum instruments for measurement of pressure and interlock of the sector valves. The small sector between the two push-pull valves will be pumped and interlocked with a mobile (removable) vacuum system.

The UHV detector and QD0 sectors will be pumped by sputter-ion pumps, with additional NEG or sublimation pumps as necessary. The post-collision line will require a high pumping speed due to the large surface area and beam-induced outgassing. A combination of sputter-ion, turbo-molecular and mechanical pumps will be used.

The post-collision line will consist of stainless steel vacuum chambers in stepped or conical forms inside the magnetic and absorber elements. As the absorbers are outside the vacuum chambers, the chambers will be designed with windows upstream of the intermediate dump absorbers and an exit window separating the collider vacuum system from the main dump body.

5.10.2.8 Overall integration

The forward region includes several important components with quite different functionalities: the final focusing magnets QD0, the Lumical and Beamcal calorimeters, the beam position monitors and kickers for the beam diagnostics and correction, the beampipe, the sensors and piezo-actuators for the active stabilization of QD0. Two independent support tubes with distinct functions and stiffness will provide the mechanical support. Both are flanged together at their extremity and cantilevered from the tunnel wall by a strong retaining bracket. This bracket has a stiff flange that allows a bolted connection to the support tube flange, a sliding pad underneath as well as the pre-alignment mechanics. The whole system sits on a pre-isolator. Figure 23 shows the detail of the connecting part between tunnel and detector whereas Figure 24 depicts in more detail the front part of the support tube. Additional integration problems arise due to the 20 mrad crossing angle of the incoming and outgoing beams. The QD0s are aligned with respect to the incoming beam. The push-pull procedures require breaking the vacuum system each time; therefore sectorization valves will be installed on the beampipe, between the QD0s and the Beamcals, for quick, safe and reliable vacuum operations.

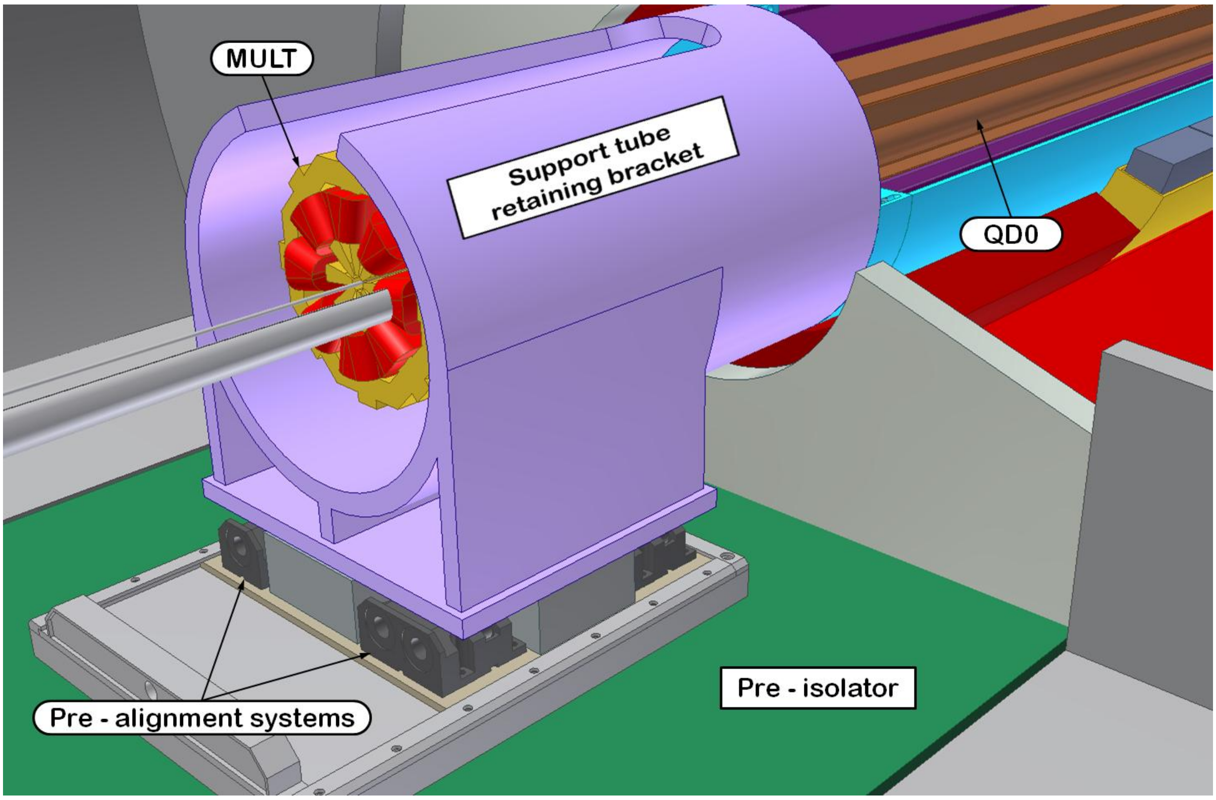

Fig. 23: Rear part of support tube with QD0, retaining bracket and pre-alignment underneath

Both detectors will move on independent platforms made of reinforced concrete with a size of ~13x16x2 m^3. The design will be similar to the plug of the PX56 shaft at CMS, which has been successfully operated and surveyed up to 2500 tons. The gross weight of the detector plus platform will be around 15,000 (13,000+2,000) tons.

The platforms will be in contact with the floor trough a set of (possibly anti-seismic) supports, which will redistribute the total load. First finite element calculations confirm that with a thickness of 2 m the local stress and deformation remain well below the permissible values.

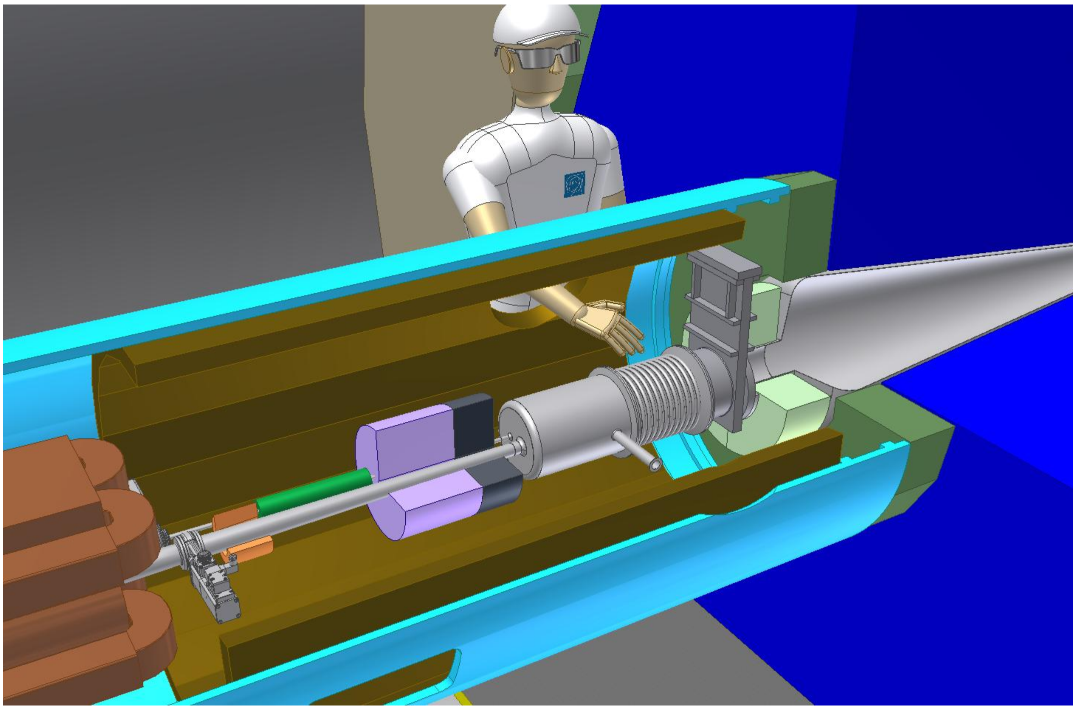

Fig. 24: Front part of support tube structure with QD0, BPM and kicker, vacuum valve, BeamCal and the transition region to the barrel parts

The moving system will be specified for moving a total mass of 15’000 tons and the option to use air pads or heavy-duty rollers is under study. The friction factor will be 1.5% and 5% respectively. In both cases, as an example, a set of pulling hydraulic strands jacks, with a sufficient capacity, commercially available, can be integrated in the design without major difficulties. A guiding rail system with indexing capability at the interaction point will also be included to achieve the required alignment precision on the beam of ±1 mm and 0.1 mrad between consecutive push-pull operations.

The floor underneath the platforms will contain deep trenches to host the cable chains and provide access for the maintenance of the air pads or the heavy-duty rollers.

5.10.2.9 Experimental Area

Apart from offering identical layout and features to the two experiments, the layout of the underground interaction region has to satisfy many requirements [15]. These include minimizing the volume to be excavated and the cost, integration of services, personnel access, ventilation, survey galleries and general safety features. At the present stage it has ben assumed that the detector will be assembled in its surface hall and lowered in large units into its underground cavern. Therefore only a crane of limited capacity (of the order of 40 tons) is foreseen in each underground area. Each experimental cavern has its own access shaft. For the moment this access shaft is situated at the extremity of the cavern outside the region covered by the opened experiment. The experiment has a diameter of ~14 m, but one has to add approximately 1.5 m on each side for the frame structure supporting external racks. With some lateral margin for the lowering, a shaft diameter of 18 m seems reasonable. Due to the fact that the elements to be lowered are much longer in one direction than in the other one, the lift, the ventilation ducts and the emergency staircase can be located inside the same shaft. Figures 25 and 26 depict the main dimensions. More details on the civil engineering aspects can be found in chapter 6.

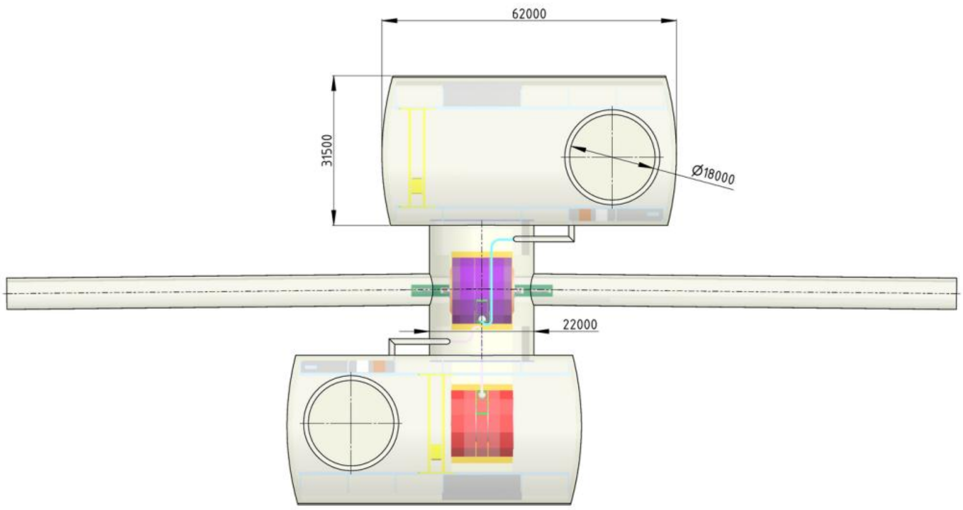

Fig. 25: Top view of the experimental area with dimensions

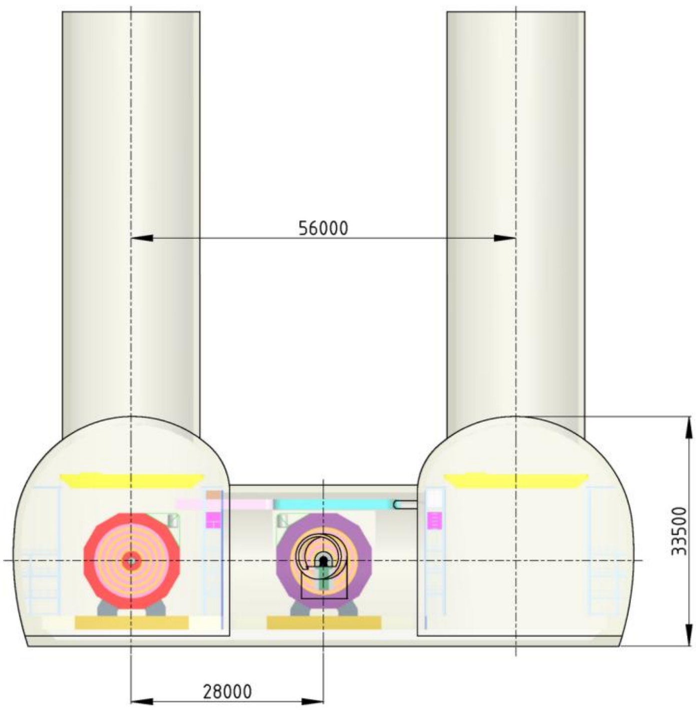

Fig. 26: Side view with dimension

5.10.3 Technical issues

There are a number of technical issues that require further work during the Technical Design phase. They concern in particular the finalization of the QD0 design and certain aspects of its stabilization and alignment. The development of the real, full-size QD0 magnet design (working in an accelerator environment and with a length of 2.73 m) is not a priority for the Conceptual Design. Nevertheless some studies to check the feasibility of a longer quadrupole, based on the proposed design, have been launched. Further work will continue in the TDR phase.

On the other hand, as the active stabilization of the magnet (like the stabilization of the ~ 4000 quadrupoles of the Main Beam) is a priority and a critical item of the CLIC R&D, more simulation studies and analysis of the mechanical behaviour of a longer magnet are necessary.

For the QD0 pre-alignment, additional work is needed to develop a method to displace the wire stretcher to the tunnel when QD0 is dismounted.

5.10.4 Component inventory

The main components of the Beam Delivery System are listed in Table 5.10.2.

Table 5.10.2 Components in the MDI region

Items	Number	Comments
QD0 magnet	4	To be replaced in case of important energy changes.
QD0 rectifiers	2x4	One rectifier per pole
QD0 stabilisation systems	2	Sensors plus piezo-actuators plus pre-isolators plus support tubes
QD0 pre-alignment systems	2	
Vacuum system	1	One Beryllium chamber in the detector region, 2 QD0 chambers plus vacuum into the post-collision beam region
IP feedback system	4	4 Beam Position Monitors, 4 kickers and associated electronics
Anti-solenoids	4	Adapted to each detector

5.10.5 Cost considerations

The Machine Detector Interface region contains a limited number of elements and most of them do not represent a large investment. One major cost item is of course the civil engineering of the experimental areas. The cost of the detectors is considered separately from the MDI.

5.10.6 Outlook for Technical Design Report phase

The proof of principle of a stabilization strategy has been validated in the laboratory with a representative prototype and with robust simulations. However, there is still important work to be carried out for the technological validation of the solution in the MDI region and its environment. The current stabilization device could be modified as new results are obtained.

IP feedback issues that require further study include the background (electromagnetic and neutron) radiation environment in the FB region, and the corresponding impact upon the radiation hardness requirements for the electronics components. Depending on the outcome, some local shielding may be required. Attention also needs to be paid to insulation against RF pickup, as well as prevention of RF broadcast into the neighbouring environment.

More work is required to incorporate two detectors with different L* values, in case this cannot be avoided. Further calculations will be done on the combined stabilization and feedback/feedforward performance.

REFERENCES

[1] K.Halbach, ‘Magnet Innovations for Linacs’, Proceedings of “1986 Linear Accelerator Conference”, SLAC-R-303, Linac86-105, TH2-1.

[2] M.Modena, Technical Specification of the CLIC Final Focus Short QD0 Hybrid Prototype, EDMS document No 1065698. See also http://indico.cern.ch/getFile.py/access?contribId=1&resId=0&materialId=slides&confId=89765

[3] B.Bolzon, ‘Etude de la stabilisation des quadrupoles de la ligne de faisceau d’un futur collisionneur linéaire’, Université de Savoie, France, 2007.

[4] L. Brunetti et al., ‘Vibration stabilization for a cantilever magnet prototype at the sub-nanometer scale’, 11th European Particle Accelerator Conference EPAC'08, Italy (2008), LAPP-TECH-2008-01.

[5] S.Redaelli, ‘Stabilization of Nanometre-Size Particle Beams in the Final Focus System of the Compact Linear Collider (CLIC)’, Université de Lausanne, Switzerland, 2003.

[6] G.Balik et al., ‘Stabilization study at the sub-nanometer level of the future Compact Linear Collider at the interaction point’, to be presented at Mecatronics 2010, Japan.

[7] Fernando Ramos, Dynamic analysis of the FF magnets pre-isolator and support system, to be published.

[8] F.Lackner et al., Development of an eccentric cam-based active pre-alignment system of the CLIC Main Beam quadrupole magnet, MEDSI2010, Oxford, UK, 2010.
H.Mainaud Durand et al, CLIC active pre-alignment system: proposal for CDR and program for TDR, IWAA 2010, Hamburg, Germany, 2010.

[9] S.Aefsky et al., The optical alignment of the ATLAS muon spectrometer endcaps, 2008 JINST 3 P11005.

[10] H.Gerwig, Novel ideas about a magnet yoke, CLIC’09 workshop, CERN, 2009, see http://indico.cern.ch/getFile.py/access?contribId=55&sessionId=8&resId=1&materialId=slides&confId=45580 .
H. Gerwig, LCD Technical Note 2010-XY, to be published.

[11] A.Gaddi, Mechanical works in magnetic stray fields, EDMS doc# 973739.

[12] P.N. Burrows et al., ‘Feedback on Nanosecond Timescales (FONT): Results from First Beam Tests at the NLCTA at SLAC’; Proceedings PAC03, Portland, Oregon, May 2003,p. 687.

P.N. Burrows et al., ‘Nanosecond timescale intra-bunch-train feedback for the linear collider: results of the FONT2 run’; Proceedings EPAC04, Lucerne, July 2004, p. 785.

[13] P.N. Burrows et al., ‘Tests of the FONT3 Linear Collider Intra-train Beam Feedback System at the ATF’, Proceedings PAC05, Knoxville, TN, May 2005, p. 1359.

[14] P.N. Burrows et al., ‘Performance of the FONT3 fast analogue intra-train beam-based feedback system at ATF’; Proceedings EPAC06, Edinburgh, UK, June 2006, p. 852.

[15] H.Gerwig, 'MDI engineering issues for a CLIC Detector', International Linear Collider Workshop, March 2010, Beijing, http://ilcagenda.linearcollider.org/getFile.py/access?contribId=50&sessionId=6&resId=0&materialId=slides&confId=4175.